

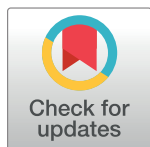
RESEARCH ARTICLE

MUC1 is a receptor for the *Salmonella* SiiE adhesin that enables apical invasion into enterocytes

Xinyue Li¹, Nancy M. C. Bleumink-Pluym¹, Yvette M. C. A. Luijkx^{1,2}, Richard W. Wubbolts³, Jos P. M. van Putten¹, Karin Strijbis^{1*}

1 Department of Infectious Diseases & Immunology, Utrecht University, Utrecht, The Netherlands, **2** Department of Chemical Biology and Drug Discovery, Utrecht Institute for Pharmaceutical Sciences and Bijvoet Center for Biomolecular Research, Utrecht University, Utrecht, The Netherlands, **3** Department of Biochemistry and Cell Biology, Utrecht University, Utrecht, The Netherlands

* K.Strijbis@uu.nl



OPEN ACCESS

Citation: Li X, Bleumink-Pluym NMC, Luijkx YMCA, Wubbolts RW, van Putten JPM, Strijbis K (2019) MUC1 is a receptor for the *Salmonella* SiiE adhesin that enables apical invasion into enterocytes. *PLoS Pathog* 15(2): e1007566. <https://doi.org/10.1371/journal.ppat.1007566>

Editor: Andreas J Baumber, University of California Davis School of Medicine, UNITED STATES

Received: September 25, 2018

Accepted: January 6, 2019

Published: February 4, 2019

Copyright: © 2019 Li et al. This is an open access article distributed under the terms of the [Creative Commons Attribution License](https://creativecommons.org/licenses/by/4.0/), which permits unrestricted use, distribution, and reproduction in any medium, provided the original author and source are credited.

Data Availability Statement: All relevant data are within the manuscript and its Supporting Information files.

Funding: The author(s) received no specific funding for this work.

Competing interests: The authors have declared that no competing interests exist.

Abstract

The cellular invasion machinery of the enteric pathogen *Salmonella* consists of a type III secretion system (T3SS) with injectable virulence factors that induce uptake by macropinocytosis. *Salmonella* invasion at the apical surface of intestinal epithelial cells is inefficient, presumably because of a glycosylated barrier formed by transmembrane mucins that prevents T3SS contact with host cells. We observed that *Salmonella* is capable of apical invasion of intestinal epithelial cells that express the transmembrane mucin MUC1. Knockout of MUC1 in HT29-MTX cells or removal of MUC1 sialic acids by neuraminidase treatment reduced *Salmonella* apical invasion but did not affect lateral invasion that is not hampered by a defensive barrier. A *Salmonella* deletion strain lacking the SiiE giant adhesin was unable to invade intestinal epithelial cells through MUC1. SiiE-positive *Salmonella* closely associated with the MUC1 layer at the apical surface, but invaded *Salmonella* were negative for the adhesin. Our findings uncover that the transmembrane mucin MUC1 is required for *Salmonella* SiiE-mediated entry of enterocytes via the apical route.

Author summary

The bacterial pathogen *Salmonella enterica* is one of the most common causes of human foodborne infection affecting millions of people worldwide each year. To establish infection, *Salmonella* needs to cross the mucus layer and invade intestinal epithelial cells from the apical surface. However, the apical surface of intestinal epithelial cells is covered with a defensive barrier of large glycosylated transmembrane mucins. These large proteins prevent contact between the *Salmonella* type III secretion needle and the host plasma membrane thereby preventing invasion. We show for the first time that MUC1, one of the intestinal apical transmembrane mucins, facilitates *Salmonella* invasion. The *Salmonella* giant adhesin SiiE is the adhesin responsible for engaging MUC1 and the interaction is mediated by glycans on MUC1. We propose that SiiE interacts with MUC1 in a zipper-like manner that involves repetitive domains in both proteins. Adhesin-receptor

interactions are essential for bacterial infection of host cells and key factors in determining target tissues and host range of bacteria. The SiiE-MUC1 invasion pathway may explain tropism of different *Salmonella* strains and provide a novel target for infection intervention and prevention.

Introduction

In the gastrointestinal tract, the luminal microbiota is separated from the underlying epithelial cells by a complex system collectively called the mucus layer. The mucus layer consists of soluble gel-forming mucins such as MUC2 and MUC5A that are secreted by Goblet cells, IgA antibodies, host defense peptides, and other anti-microbial components [1]. Another component of the mucus layer are transmembrane mucins, which are large glycoproteins that are expressed on the apical surface of enterocytes and Goblet cells. Transmembrane mucins expressed in the gastrointestinal tract include MUC1, MUC3A, MUC3B, MUC4, MUC12, MUC13, MUC15, MUC17, MUC20 and MUC21 [2]. Transmembrane mucins have a highly glycosylated extracellular domain with potential barrier function, a transmembrane domain and a cytoplasmic tail that links to signaling pathways [3].

MUC1 is the most extensively studied transmembrane mucin and is highly expressed at mucosal surfaces including the stomach and the intestinal tract [4,5]. The MUC1 extracellular domain forms a large filamentous structure with a variable numbers of tandem repeats (VNTR) domain that can protrude 200–500 nm from the plasma membrane [6,7]. The extracellular domain is highly O-glycosylated with complex sugars that frequently terminate with sialic acids or fucose [8]. The human and mouse MUC1 extracellular domains share less than 40% homology while the transmembrane domain and cytoplasmic tail are highly conserved [9].

MUC1 plays an important role in defense against invasive bacterial pathogens such as *Helicobacter pylori* and *Campylobacter jejuni*. *In vitro* experiments with *H. pylori* and a gastrointestinal cell line showed that the extracellular domain of MUC1 is released and acts as a decoy that prevents bacterial attachment to cells [10]. Overexpression of MUC1 in HeLa cells or HCT116 cells protects against *C. jejuni* Cytotolethal Distending Toxin (CDT) and CDT-treated cells internalize MUC1 into cytoplasmic vesicles or into the nucleus [11]. Expression of MUC1 in HCT116 cells increased adherence of *C. jejuni*, but invasion was not affected by MUC1 expression. The authors showed that *C. jejuni* adheres to O-glycan H type 2 sugars that contain a terminal fucose group [11]. In *in vivo* infection experiments, Muc1 knockout mice showed increased susceptibility to *H. pylori* and *C. jejuni* with more severe epithelial damage [10–12], but did not display increased susceptibility to *Salmonella* Typhimurium infection [11]. In addition to bacterial pathogens, MUC1 (over)expression also reduced infection by adenoviruses and influenza A [13–15].

Salmonella enterica is a food-borne, motile and facultative gastrointestinal pathogen. The non-typhoidal *Salmonella* (NTS) strains, *S. enterica* subsp. *enterica* serovar Enteritidis (*S. Enteritidis*) and *S. enterica* subsp. *enterica* serovar Typhimurium (*S. Typhimurium*) can cause self-limiting gastroenteritis in a wide range of hosts [16]. Three main routes have been described for *Salmonella* mucosal invasion: entry through M cells, direct invasion of enterocytes, and uptake through dendritic cells [17]. *Salmonella* cellular invasion is mediated by a type III secretion system that injects virulence factors into host cells to induce uptake. This process is well-studied for *Salmonella* invasion of different types of epithelial cells [18]. During intestinal pathogenesis *Salmonella* encounters the apical surface of intestinal epithelial cells

where invasion is less efficient due to a defensive barrier of glycosylated transmembrane mucins. The transmembrane mucins presumably prevent contact of the T3SS with the host plasma membrane. The *Salmonella* giant adhesin SiiE that is secreted by the T3SS and encoded by Pathogenicity Island 4 (SPI4) has been shown to be a key factor in apical invasion of polarized epithelial cells [19,20]. A specific receptor for SiiE that enables *Salmonella* apical entry has not been identified. In this study, we investigate the role of transmembrane mucin MUC1 during *Salmonella* invasion into intestinal epithelial cells.

Results

Salmonella apical invasion of intestinal epithelial cells coincides with MUC1 expression

Various human intestinal epithelial cell lines derived from colorectal carcinomas are used to study interactions with enteric pathogens, e.g. Caco-2, HT-29, HT29-MTX and HRT-18 cells. Previously it was shown that *Salmonella* apical adhesion and invasion is more effective in HT29-MTX cells compared to Caco-2 or HT-29 cells [21]. For this reason, we selected HT29-MTX cells to study the function of MUC1 during *Salmonella* invasion. To investigate MUC1 expression in HT29-MTX cells, we grew the cells for 5 days to form a confluent monolayer and performed immunofluorescence confocal microscopy with the 214D4 antibody directed against the MUC1 extracellular domain. MUC1 was expressed in a high percentage of HT29-MTX cells and localized to the apical side in an island-like pattern (Fig 1A).

To facilitate confocal microscopy of *Salmonella* invasion, we used *S. Enteritidis* containing a plasmid encoding red fluorescent mCherry. *S. Enteritidis* was grown till late logarithmic phase to achieve a high motile state and co-incubated with confluent HT29-MTX cells for 1 h. In this experimental setup, only the apical surface of the HT29-MTX cells is exposed to *Salmonella*. As revealed by confocal microscopy, *S. Enteritidis* invaded and formed clusters predominantly in MUC1 positive cells and did not invade adjacent MUC1-negative cells (Fig 1B). MUC1 seemed to localize to cup-like structures that contained large *Salmonella* clusters (Fig 1B). Multiple Z-stacks of the image were collected, and an orthogonal view clearly showed apical MUC1 with clusters of *Salmonella* located underneath (Fig 1C and S1A and S1B Fig). MUC1 did not colocalize with the intracellular *Salmonella*. Next, we investigated the contribution of the T3SS to apical invasion of HT29-MTX cells with a *Salmonella* Enteritidis CVI-1 wild type strain and its isogenic mutant *invG*, that is deficient in T3SS-mediated invasion. While the wild type strain did invade HT29-MTX cells at MUC1-positive loci, no adherent or invaded *invG* mutant bacteria could be detected (S1C Fig).

To determine if this phenomenon is restricted to *S. Enteritidis*, we also tested *S. Typhimurium*, another non-typhoidal *Salmonella*. We used *S. Typhimurium* containing a plasmid encoding GFP [22,23] and co-incubated the bacteria with confluent HT29-MTX cells. Comparable to *S. Enteritidis*, *S. Typhimurium* invaded and formed clusters in MUC1-expressing cells while MUC1-negative cells remained uninfected (Fig 1D). Again, MUC1-positive cup-like structures containing *Salmonella* clusters were observed. From these data we hypothesize that MUC1 positively contributes to the apical invasion of different *S. enterica* serovars into HT29-MTX cells.

Generation of MUC1 knockout cells

To determine the role of MUC1 in *S. Enteritidis* entry, we firstly designed a CRISPR/Cas9 genome editing strategy to knock out MUC1 in HT29-MTX cells (Fig 2A). Two guide RNAs (gRNAs) were selected in the 5' end of the MUC1 gene that would generate a 130 bp deletion

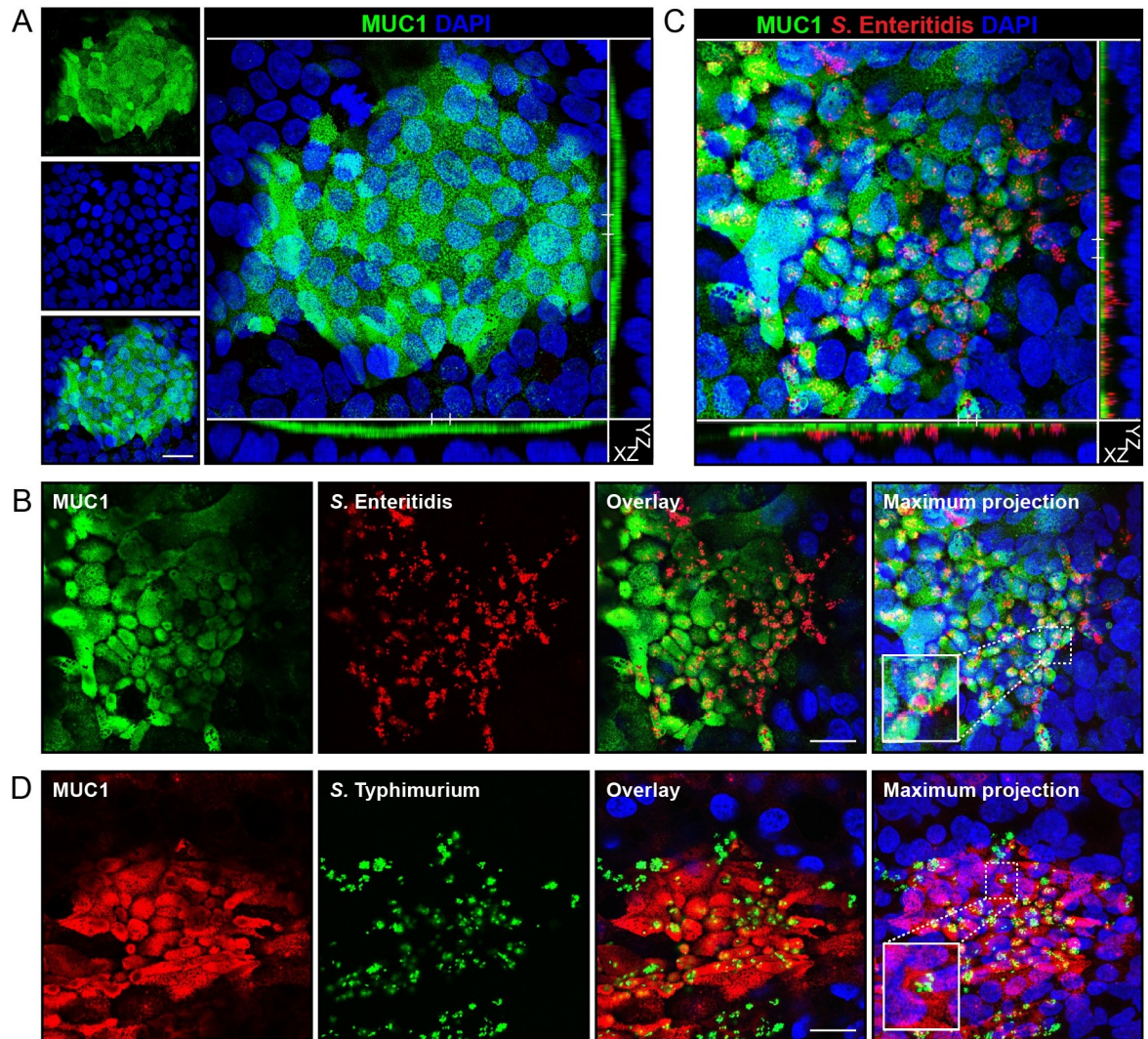


Fig 1. *Salmonella* invades intestinal HT29-MTX cells that express MUC1. (A) Immunofluorescence confocal microscopy imaging of confluent HT29-MTX cells with anti-MUC1 antibody 214D4 (green) and DAPI to stain the nuclei (blue). (B, C) Immunofluorescence confocal microscopy infection experiment with confluent HT29-MTX cells and *Salmonella enterica* Enteritidis (mCherry, red) at MOI 60 for 1 hour stained with anti-MUC1 214D4 antibody (green) and DAPI to stain the nuclei (blue). (D) Infection experiment with confluent HT29-MTX cells and *Salmonella enterica* Typhimurium (GFP, green) at MOI 60 for 1 hour stained with anti-MUC1 214D4 antibody (red) and DAPI (blue). White scale bars represent 20 μ m.

<https://doi.org/10.1371/journal.ppat.1007566.g001>

before the start of the tandem repeats. After transfection with the CRISPR-2xgRNA plasmid, cells were selected with puromycin and a positive single cell clone with the 130 bp deletion was identified (HT29-MTX- Δ MUC1; Fig 2B). Western blot analysis of wild type HT29-MTX cells revealed a reactive band of approximately 460 kDa that most likely represents fully glycosylated MUC1 and a band of about 170 kDa that presumably represents the unglycosylated precursor. Both bands were absent in the Δ MUC1 cells (Fig 2C).

MUC1 facilitates *S. Enteritidis* apical entry of intestinal epithelial cells

Next, we performed *Salmonella* apical invasion experiments with the wild type and Δ MUC1 monolayers followed by confocal microscopy. *S. Enteritidis* invaded and formed clusters in the

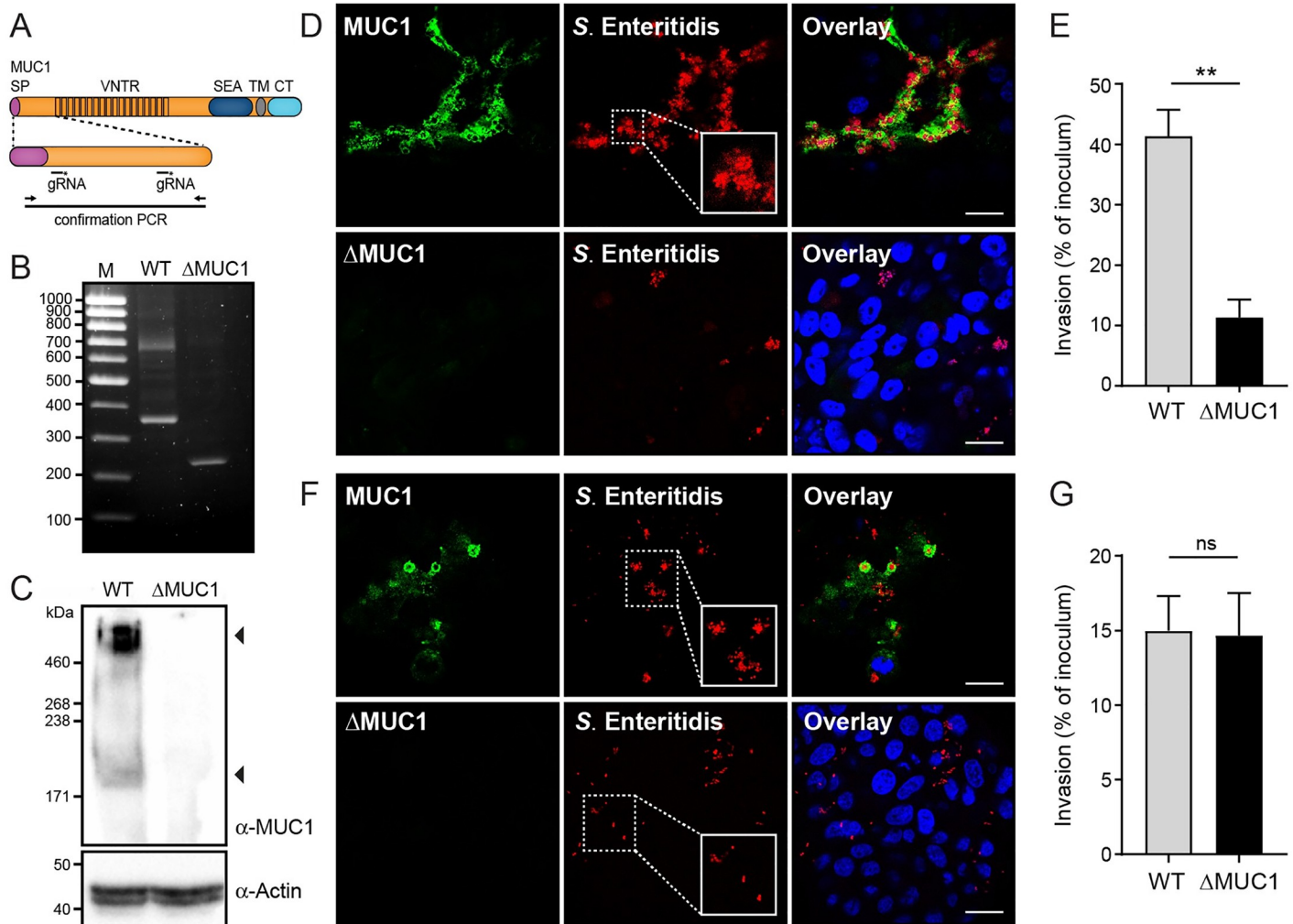


Fig 2. Knockout of MUC1 reduces *S. Enteritidis* apical invasion. (A) Schematic representation of the MUC1 coding region with different domains and the position of the guide RNAs (gRNAs) to generate a genetic deletion. SP, signal peptide; VNTR, variable numbers of tandem repeats; SEA, sea urchin sperm enterokinase agrin domain; TM, transmembrane domain; CT, cytoplasmic tail. The position of the deletion confirmation PCR primers is indicated. (B) Confirmation PCR of wild type HT29-MTX (WT) and HT29-MTX MUC1 knockout cells (Δ MUC1). (C) Western blot analysis of HT29-MTX wild type (WT) and MUC1 knockout cells (Δ MUC1) stained for MUC1 (214D4 antibody) or Actin. (D) Immunofluorescence confocal microscopy imaging showing apical invasion of confluent HT29-MTX wild type and Δ MUC1 cells after *S. Enteritidis* infection (1h) at MOI 60. MUC1 antibody 214D4 was used to stain MUC1 (green) and DAPI was used to stain nuclei (blue). (E) Quantification of *S. Enteritidis* invasion into confluent HT29-MTX wild type and Δ MUC1 cells. Confluent cells were incubated with *S. Enteritidis* for 1h at MOI 15 and subsequently treated with gentamicin (300 μ g/ml). Cells were lysed and surviving intracellular bacteria were quantified by colony counts. Invasion is expressed as percentage of initial inoculum. Values are the mean \pm SEM of three independent experiments performed in triplicate. (F) Immunofluorescence confocal microscopy imaging showing invasion of non-confluent HT29-MTX wild type and Δ MUC1 cells after *S. Enteritidis* infection as described under A. (G) Quantification of *S. Enteritidis* invasion into non-confluent HT29-MTX wild type and Δ MUC1 cells as described under E. Statistical analysis was performed by Student's *t*-test using GraphPad Prism software. * $p < 0.05$; ** $p < 0.01$; ns, not significant. White scale bars represent 20 μ m.

<https://doi.org/10.1371/journal.ppat.1007566.g002>

wild type cells as described above, but the bacteria barely invaded the Δ MUC1 cells (Fig 2D). To quantify this difference, we performed a quantitative invasion assay in which extracellular bacteria are killed with gentamicin and viable internalized bacteria are counted. This assay showed that approximately 41% of the introduced *S. Enteritidis* invaded the wild type cells, while about 11% of the bacteria invaded Δ MUC1 cells ($p < 0.01$) (Fig 2E). The quantitative assay yielded a less pronounced effect compared to the microscopy. We hypothesize that this discrepancy is due to false positives in the quantification assay, a known problem associated with such assay that might be more pronounced during invasion at the apical surface. These

data indicate that MUC1 does not form a barrier for *Salmonella* invasion but facilitates apical entry into HT29-MTX cells.

As *Salmonella* utilizes different strategies for apical or (baso)lateral invasion into intestinal epithelial cells, we also carried out invasion assays with 2-day grown non-confluent HT29-MTX WT and Δ MUC1 cells. These cells formed small islands with exposed lateral sides on the rim. MUC1 was only expressed in a limited number of cells in the center of the island. *S. Enteritidis* invaded both wild type and Δ MUC1 cell islands but showed a very different pattern. The large *S. Enteritidis* clusters described above were found exclusively in MUC1-expressing cells. A high percentage of Δ MUC1 cells was infected with *S. Enteritidis* through the lateral route, but only small red puncta of single bacteria could be observed (Fig 2F). In the apical invasion experiments with the confluent monolayers such small puncta were not observed. A quantitative invasion assay with non-confluent cells showed no difference in *S. Enteritidis* invasion between wild type and Δ MUC1 cells (Fig 2G). The formation of *Salmonella* clusters during apical invasion was previously described and only occurs in areas of membrane ruffle formation and macropinocytosis [24]. Our data suggest that MUC1 is associated with this apical process and that lateral invasion of *Salmonella* that is independent of MUC1 results in a different outcome. Collectively, these data demonstrate that MUC1 is an essential component for apical invasion of *S. Enteritidis* into confluent HT29-MTX cells but is not required for lateral entry of *S. Enteritidis* into non-polarized cells. Apical invasion through MUC1 appears to be very efficient and results in uptake of large clusters of *Salmonella* while individual bacteria internalize during lateral invasion.

***Salmonella* invades different intestinal epithelial cell lines that express MUC1**

To further substantiate the MUC1 contribution to *Salmonella* invasion, we performed apical invasion assays with early confluent monolayers of HT-29, Caco-2 and HRT-18 intestinal epithelial cell lines. Confocal microscopy showed that, under these conditions, HT-29, Caco-2 and HRT-18 cells express relatively low levels of MUC1 compared to HT29-MTX cells. Immunoblot analysis to determine MUC1 expression level in all cell lines indicated clear MUC1 bands in HT29-MTX and HT-29 cells, whereas MUC1 expression was below detection level in the other two cell lines after 5 days of culture (Fig 3A). Invasion assays showed that *Salmonella* did invade and form clusters in the MUC1-positive cells in the different cell lines although invasion levels seemed lower than detected for HT29-MTX cells (Fig 3B). MUC1 is reported to be upregulated under inflammatory conditions, for example after exposure to IL-6 [25,26]. Treatment of the early confluent monolayers with IL-6 strikingly increased MUC1 expression in HT29-MTX cells and HT-29 cells, but no difference was observed for Caco-2 and HRT-18 cells (Fig 3A). These results demonstrate variable MUC1 expression between cell lines and conditions and explain differences in apical invasion behavior of the pathogen between different intestinal epithelial cell lines.

The interaction of *Salmonella* with MUC1 is mediated by sialic acids

Alpha-2,3-linked sialic acids are essential for apical invasion of *S. Typhimurium* into MDCK cells [20]. The tandem repeats of the MUC1 extracellular domain are highly glycosylated with complex O-linked glycans on which sialic acids are frequently present [8]. To investigate if sialic acids on MUC1 are involved in apical invasion of *S. Enteritidis* into HT29-MTX cells, we removed α 2,3-, α 2,6-, and α 2,8-linked sialic acids by neuraminidase treatment prior to the addition of *Salmonella*. Confocal microscopy showed that neuraminidase treatment of the HT29-MTX wild type cells resulted in a reduced *S. Enteritidis* invasion into wild type cells and

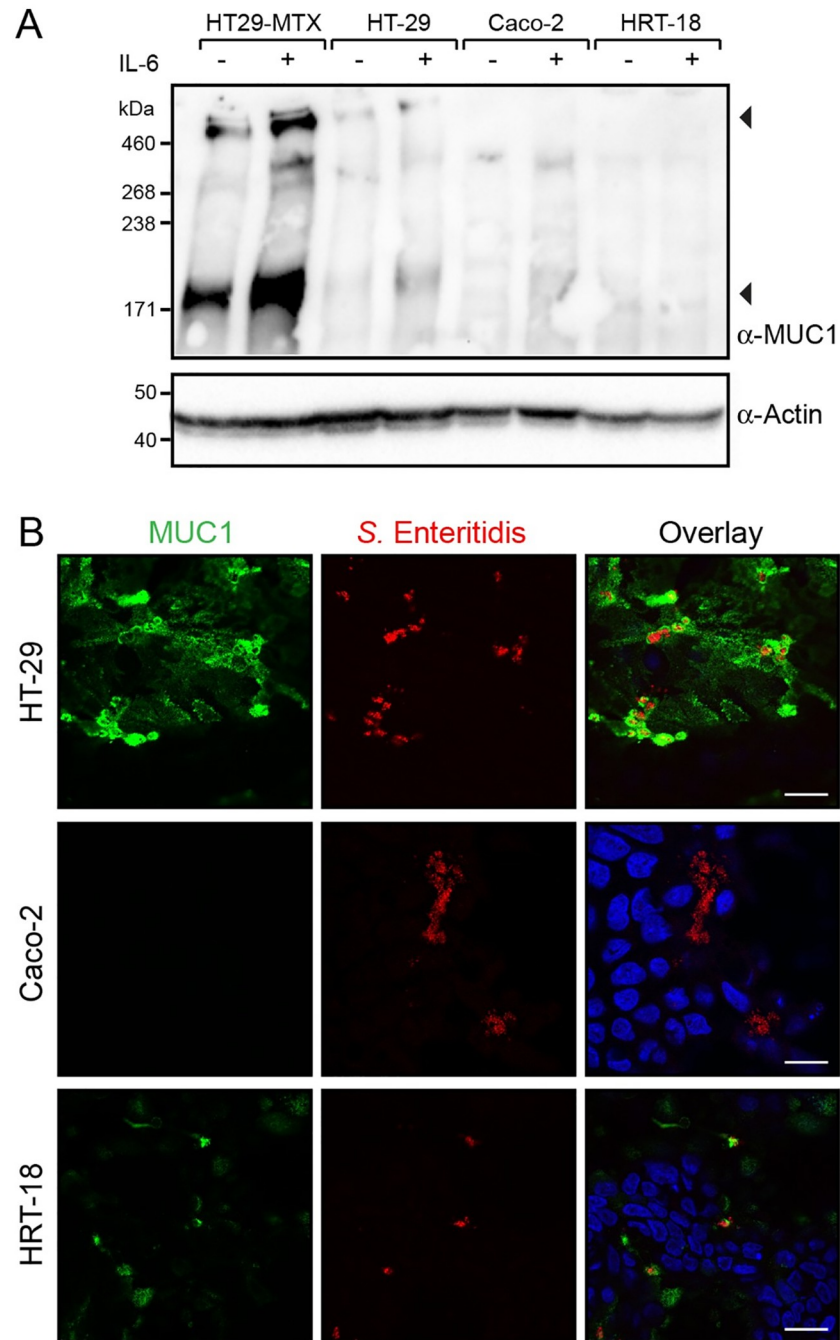


Fig 3. MUC1 expression and *Salmonella* invasion in different intestinal epithelial cell lines. (A) Western blot analysis of MUC1 expression levels in 5-day grown early-confluent intestinal epithelial cell lines incubated with or without the pro-inflammatory cytokine IL-6 at 100 ng/ml for 24h. (B) Immunofluorescence confocal microscopy imaging of 5-day grown early-confluent intestinal epithelial cell lines HT29-MTX, HT-29, Caco-2 and HRT-18 cells incubated with *S. Enteritidis* (mCherry, red) at MOI 60 for 1h stained with anti-MUC1 214D4 antibody (green) and DAPI (blue). White scale bars represent 20 μ m.

<https://doi.org/10.1371/journal.ppat.1007566.g003>

a disappearance of *Salmonella* clusters (Fig 4A). Neuraminidase treatment did not affect *Salmonella* apical invasion into Δ MUC1 cells (Fig 4B). The quantitative invasion assay confirmed the significant reduction in *S. Enteritidis* invasion into wild type cells after neuraminidase treatment, whereas no significant difference was observed for Δ MUC1 cells (Fig 4B). Again, we did see that the quantitative assay yielded a less pronounced effect compared to the microscopy. Together these data clearly indicate that sialic acids on the extracellular domain of MUC1 are crucial for apical entry of *S. Enteritidis* into intestinal epithelial cells.

The *Salmonella* adhesin SiiE is responsible for MUC1-mediated apical invasion

S. enterica binding to receptors on epithelial cells is mediated by different adhesins. SiiE is a giant adhesin that mediates binding of *Salmonella* to the apical side of epithelial cells [19,27]. To determine if SiiE is the adhesin that contributes to binding of MUC1, we generated a *S. Enteritidis* *siiE* knockout strain. This strain demonstrated the same growth rate as the wild type strain. Wild type and *siiE* knockout bacteria were used in apical invasion assays with confluent HT29-MTX wild type cells. As shown by microscopy, the *siiE* knockout bacteria failed to invade HT29-MTX wild type cells (Fig 5A). To exclude the possibility that deletion of *siiE* affects *Salmonella* motility, we also performed a lateral invasion assay with non-confluent cells. Under these conditions, the wild type bacteria invaded from both the lateral side and the apical surface and the latter was associated with internalization of large bacterial clusters. The *siiE* knockout bacteria did invade the cells but no large bacterial clusters were detectable (Fig 5B). These data suggest that invasion through MUC1 was completely abolished in the *siiE* mutant bacteria. Quantification of *Salmonella* infection showed that invasion of the *siiE* mutant into HT29-MTX wild type cells was significantly reduced compared to *S. Enteritidis* wild type bacteria ($p < 0.05$) (Fig 5C). Invasion of the *siiE* mutant into Δ MUC1 cells was low and not significantly altered (Fig 5C). Together, these data demonstrate that both MUC1 and SiiE are essential components for efficient apical entry of intestinal epithelial cells by *Salmonella*.

The SiiE-MUC1 *Salmonella* invasion pathway enables apical invasion of intestinal epithelial cells

It has been reported previously that *Salmonella* secretes SiiE into the culture medium, but that the adhesin remains attached to the bacterial cell wall when contacting host cells [19]. In order to further investigate the function of SiiE during MUC1-mediated apical invasion we performed immunofluorescence confocal microscopy with an antibody directed against SiiE (kindly provided by Michael Hensel). As in our previous invasion experiments, *Salmonella* invaded MUC1-positive cells and the bacteria could be observed underneath the MUC1 surface. While SiiE-positive bacteria were closely associated with the MUC1 layer, *Salmonella* that had invaded further into the epithelial cells were negative for SiiE (Fig 6A, S2 Fig). SiiE-positive *Salmonella* associated closely with the MUC1-positive cups (Fig 6B). To visualize the process of SiiE-MUC1 mediated *Salmonella* invasion in more detail, we generated a 3D projection and an accompanying movie that includes a rotation (Fig 6C and S1 Movie). Using Imaris software, we determined the position of SiiE-positive and *Salmonella*-positive spots relative to the MUC1 surface layer in 5 independent Z-stacks. The SiiE-positive spots closely associated with the MUC1 layer, while the *Salmonella* spots localized close to the MUC1 layer and deeper into the cells (Fig 6D), conforming that invaded *Salmonella* are negative for SiiE. Together, our data show that glycosylated MUC1 acts as a receptor for *Salmonella* SiiE and enables SiiE-dependent apical invasion into the intestinal epithelium (Fig 7A).

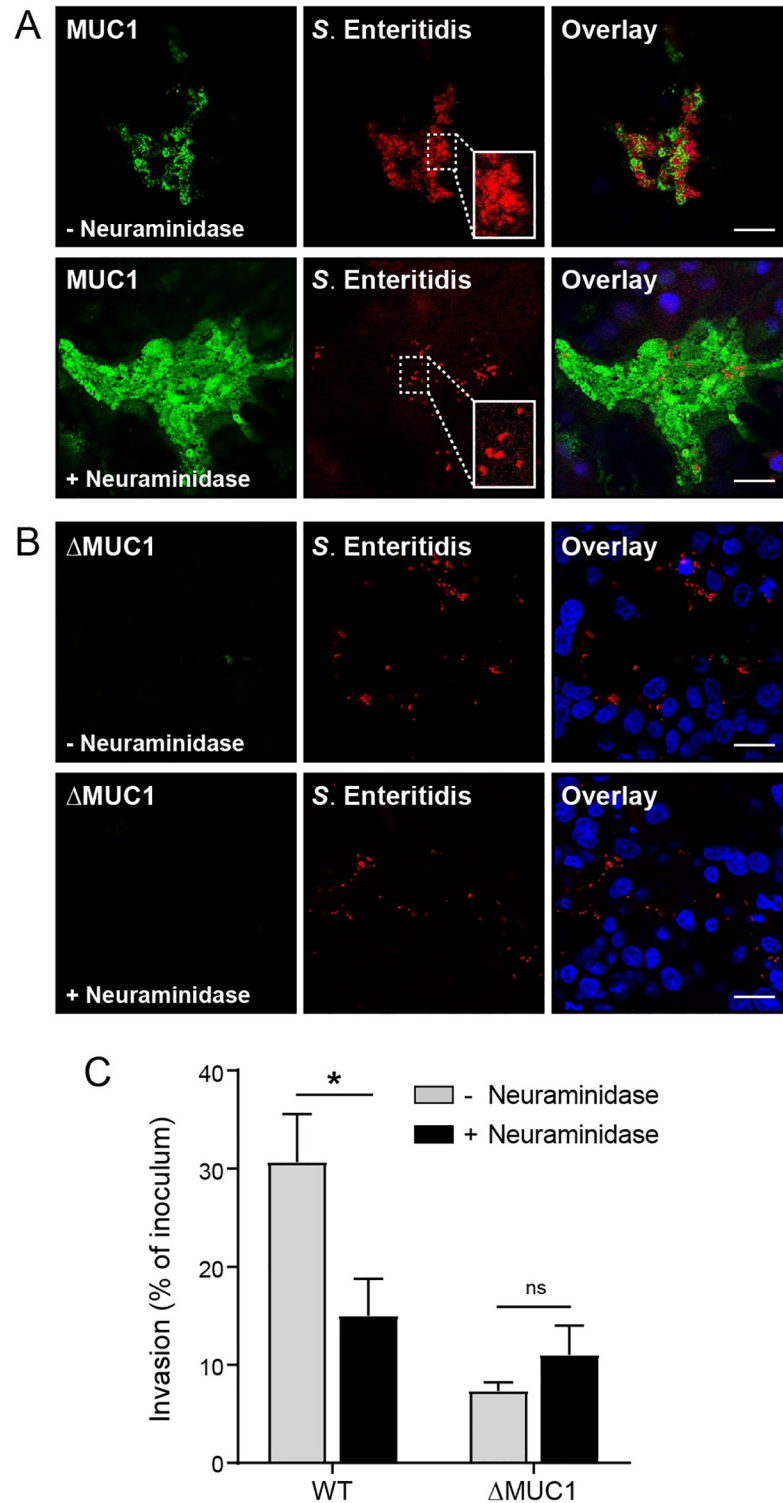


Fig 4. Deglycosylation with neuraminidase reduces *S. Enteritidis* apical invasion. Confluent HT29-MTX cells were treated with 250 mU/ml neuraminidase or DPBS for 2h followed by incubation with *S. Enteritidis* for 1 hour. (A) Immunofluorescence confocal microscopy images of confluent deglycosylated HT29-MTX cells incubated with *S. Enteritidis* (mCherry, red) stained for MUC1 (214D4, green) and nuclei (DAPI, blue). (B) Immunofluorescence confocal microscopy images of confluent deglycosylated Δ MUC1 cells incubated with *S. Enteritidis* (mCherry, red) stained for MUC1 (214D4, green) and nuclei (DAPI, blue). (C) Quantification of invaded intracellular *S. Enteritidis* in

confluent HT29-MTX wild type and Δ MUC1 cells with and without neuraminidase treatment. After neuraminidase treatment, cells were incubated with *S. Enteritidis* for 1h at MOI 15 and subsequently treated with gentamicin (300 μ g/ml). Cells were lysed and surviving intracellular bacteria were quantified by colony counts. Invasion is expressed as percentage of initial inoculum. Values are the mean \pm SEM of three independent experiments performed in triplicate. Statistical analysis was performed by Student's *t*-test using GraphPad Prism software. * $p < 0.05$; ns, not significant. White scale bars represent 20 μ m.

<https://doi.org/10.1371/journal.ppat.1007566.g004>

Discussion

Excellent work has shown that *Salmonella* T3SS enables cellular invasion, but bacterial entry into intestinal epithelial cells via the apical route appear less efficient due to a defensive barrier formed by transmembrane mucins. We demonstrate for the first time that *Salmonella* utilizes the transmembrane mucin MUC1 as a receptor to breach the apical barrier of intestinal epithelial cells. *Salmonella* efficiently invaded the apical surface of a monolayer of intestinal cells with high MUC1 expression whereas apical invasion into MUC1 knockout cells and cell lines that expressed low levels of MUC1 was severely reduced (Figs 2 and 3). Lateral invasion of non-confluent cells is not hampered by a defensive mucin layer and does not require MUC1 for entry (Fig 2). Enzymatic removal of sialic acids from intestinal epithelial cells reduced *Salmonella* invasion to MUC1 knockout levels, showing that sialic acids are instrumental for the MUC1-*Salmonella* interaction (Fig 4). MUC1-mediated invasion was abolished after the knock out of the *Salmonella* giant adhesin SiiE (Fig 5). SiiE-positive *Salmonella* closely associated with the MUC1 layer on the surface and invaded *Salmonella* were negative for SiiE (Fig 6). We propose that the SiiE-MUC1 invasion route is crucial to breach the epithelial mucin barrier and enable *Salmonella* apical invasion into MUC1-expressing enterocytes. A T3SS-1 mutant was unable to adhere or invade through MUC1, demonstrating that both the SiiE-MUC1 interaction and a functional T3SS are instrumental for successful *Salmonella* apical invasion.

Our data provide evidence that glycosylated MUC1 serves as a receptor for intestinal infection in several non-typhoid *Salmonella enterica* serovars. Different transmembrane mucins are expressed on the apical surface of intestinal epithelial cells and are generally considered to form a defensive barrier. The large filamentous glycoprotein MUC1 is widely expressed in mucosal tissues. Within the gastrointestinal tract, it is expressed in the stomach, duodenum and colon [2]. Previously, it was shown that MUC1 plays an important role in defense against the common enteric pathogens *H. pylori* and *C. jejuni* [10–12]. In contrast, our results showed that *Salmonella* exploits MUC1 for apical invasion into enterocytes. It is conceivable that other bacteria also make use of MUC1 for adhesion and invasion into host cells. For example, it has been reported that knockdown of MUC1 decreases invasion of *Staphylococcus aureus* into human corneal-limbal epithelial (HCLE) cells [28]. On the other hand, knockdown of the very long transmembrane mucin MUC16 increased invasion of *S. aureus*, suggesting that some mucin types have a barrier function for this bacterium. As the MUC protein family consists an array of transmembrane proteins with different extracellular and intracellular domains, it can be imagined that pathogens have evolved distinct strategies to breach the mucus layer and colonize the host.

The importance of MUC1 for *Salmonella* invasion via the apical route was further underpinned by the variable *Salmonella* entry in several commonly used intestinal epithelial cell lines. *Salmonella* apical infection efficiency clearly coincided with the level of MUC1 expression by these cell types. In non-polarized cells, *Salmonella* was capable of lateral invasion via a MUC1-independent route. These findings indicate that *Salmonella* can invade a single cell type through different mechanisms, dependent on the cell polarization status. We hypothesize

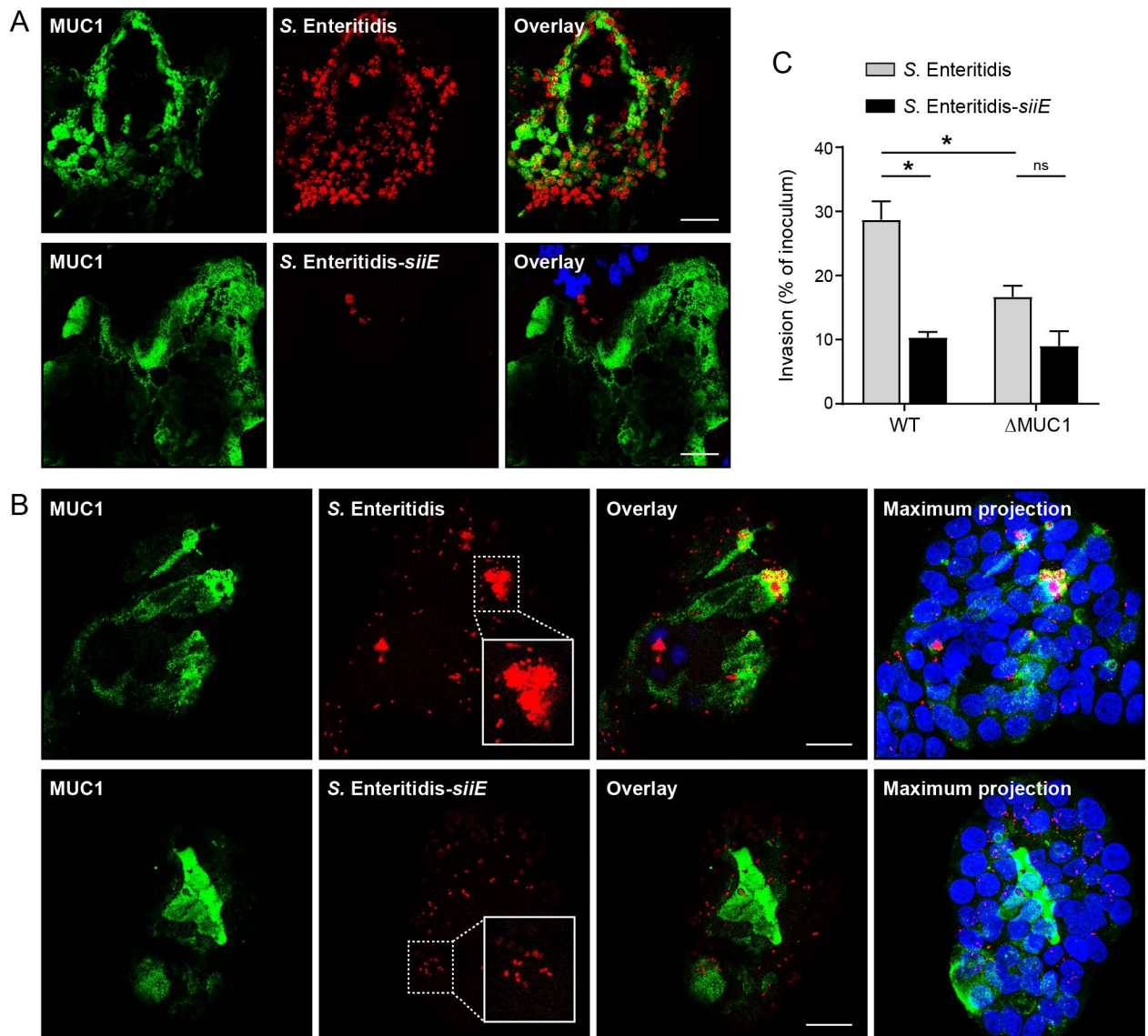


Fig 5. The *Salmonella* SiiE adhesin is responsible for MUC1-mediated invasion. (A) Immunofluorescence confocal microscopy imaging of confluent HT29-MTX cells infected with *S. Enteritidis* wild type and *siiE* knockout bacteria (mCherry, red) stained for MUC1 (214D4, green) and nuclei (DAPI, blue). (B) Immunofluorescence confocal microscopy imaging as above with non-confluent HT29-MTX cells. (C) Quantification of invaded intracellular *S. Enteritidis* wild type and *siiE* knockout bacteria. Confluent HT29-MTX cells were incubated with *S. Enteritidis* for 1h at MOI 15 and subsequently treated with gentamicin (300 μg/ml). Cells were lysed and surviving intracellular bacteria were quantified by colony counts. Invasion is expressed as percentage of initial inoculum. Values are the mean ± SEM of three independent experiments performed in triplicate. Statistical analysis was performed by Student's *t*-test using GraphPad Prism software. * $p < 0.05$; ns, not significant. White scale bars represent 20 μm.

<https://doi.org/10.1371/journal.ppat.1007566.g005>

that the SiiE-MUC1 interaction precedes contact of the T3SS with the host plasma membrane (see below).

Salmonella has been reported to exploit different mechanisms to invade the intestinal mucosa: (i) invasion through enterocytes, (ii) entry through M cells and (iii) uptake by mucosal dendritic cells [17]. It is conceivable that these seemingly redundant invasion mechanisms serve to colonize different regions of the gut and/or different species. Mouse and rabbit studies show that entry through M cells is a major route of *Salmonella* invasion [29,30]. *In vivo* studies in rabbits, calves and pigs have emphasized the importance of enterocyte invasion in addition

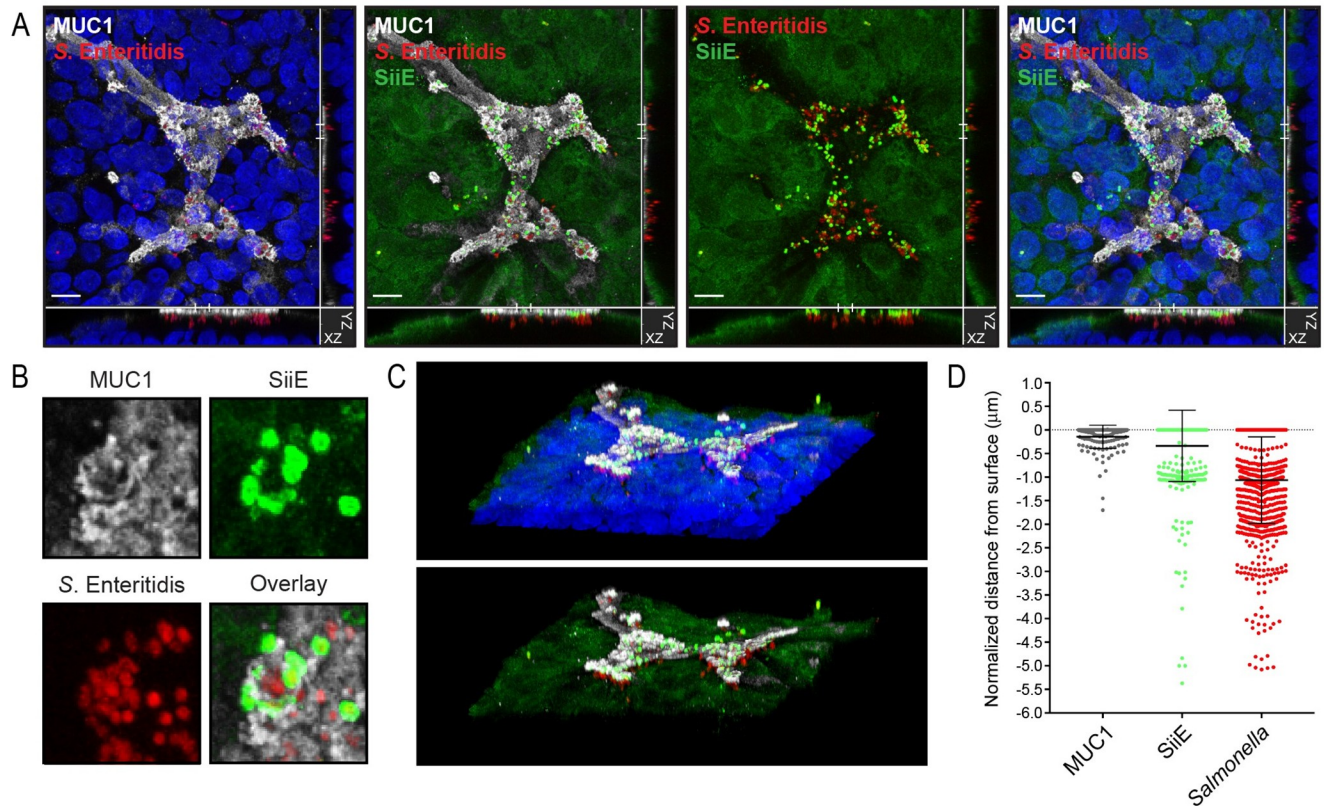


Fig 6. SiiE-positive *Salmonella* closely associate with MUC1 at the apical surface while invaded *Salmonella* are negative for SiiE (A) Immunofluorescence confocal microscopy imaging of confluent HT29-MTX cells infected with *S. Enteritidis* wild type bacteria (mCherry, red) stained for SiiE (polyclonal anti-SiiE, green), MUC1 (214D4, white) and nuclei (DAPI, blue). (B) Immunofluorescence confocal microscopy imaging detail showing localization of SiiE-positive bacteria (mCherry and green) on MUC1-positive cup-like structures (white). Bacteria inside the cup are negative for SiiE. (C) 3D projection of confocal microscopy image depicted in A. (D) Quantification and localization of SiiE-positive spots (green) and *Salmonella*-positive spots (red) relative to the MUC1-positive cellular surface using IMARIS software. White scale bars represent 20 µm.

<https://doi.org/10.1371/journal.ppat.1007566.g006>

to M cells [31–33]. To our knowledge, it is not known if M cells express MUC1. Moreover, MUC1 differs in composition and expression between species which theoretically may impact the preferred route of *Salmonella* invasion and tropism. For example, mouse Muc1 shares less than 40% homology with human MUC1 in the extracellular domain [9] and the pattern of protein glycosylation along the GI tract is opposite between mice and men. In humans, fucose decreases and sialic acid increases from ileum to colon [34], whereas in mice sialylated structures are the dominant terminal sugars in the small intestine and terminal fucose is more prevalent in the colon [35]. These differences may explain the need for different invasion routes but also make it complex to extrapolate results and to identify the predominant route of *Salmonella* invasion in different niches and species.

We identified the bacterial SiiE protein as the primary *Salmonella* adhesin involved in MUC1-mediated apical invasion. Genetic inactivation of the *siiE* gene reduced *Salmonella* entry from the apical side (Fig 5). The SiiE protein is expressed by most *S. enterica* serovars, but is a pseudogene in some highly host-adapted serotypes including *S. Typhi* [36]. The protein is encoded by *Salmonella* Pathogenicity Island 4 (SPI4) and secreted through a type I secretion system (T1SS) [19]. Association of SiiE with the bacterial surface is regulated by contact with polarized epithelial cells [37] and the protein interacts with MDCK cells in a lectin-like manner [20]. The sensitivity of the SiiE-mediated invasion for neuraminidase treatment

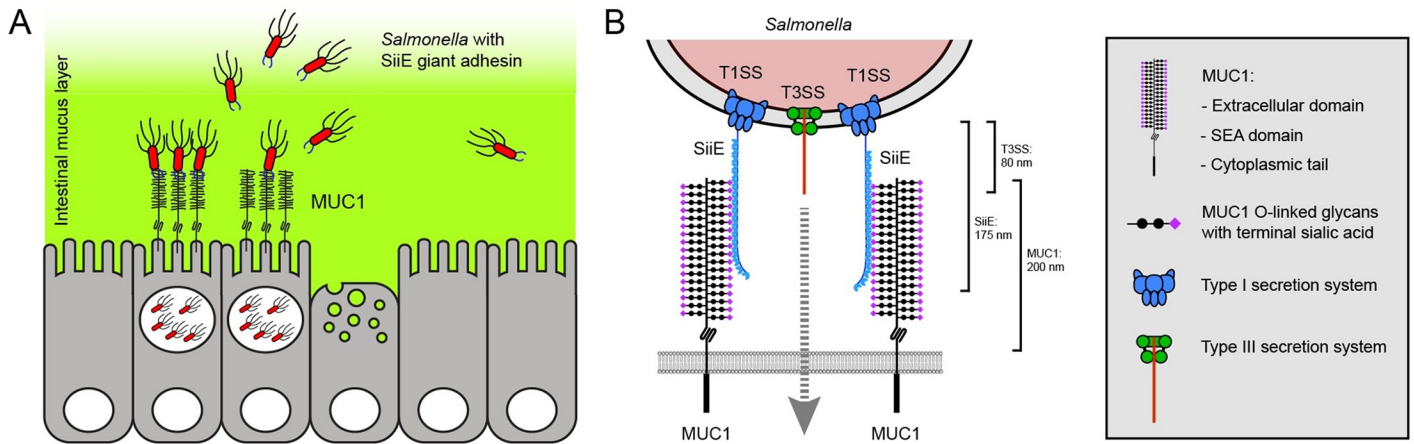


Fig 7. Schematic model showing the SiiE-MUC1 apical invasion pathway. (A) MUC1 is expressed on the apical surface of intestinal epithelial cells. *Salmonella* breaches the soluble mucus layer (green) and uses the giant adhesin SiiE to attach to MUC1 and invade the epithelial cells. After MUC1-SiiE-mediated invasion, large SiiE-negative *Salmonella* clusters are observed in the infected cells. (B) Hypothetical structural model of the SiiE-MUC1 interaction during *Salmonella* apical invasion of intestinal epithelial cells based on the molecular sizes of the involved players. The needle-like type III secretion system (T3SS) injectosome is essential for *Salmonella* invasion but is only 80 nm in length. The large transmembrane mucin MUC1 extends 200 nm from the cell surface and contains an extracellular domain with 42 tandem repeats that are highly decorated with O-linked glycans with terminal sialic acids. The giant adhesin SiiE is 175 nm in size and secreted through the type I secretion system (T1SS). SiiE contains 53 Blg repeats with sugar-binding capacity. Our data show that MUC1, sialic acids and SiiE are essential in mediating apical entry of *Salmonella*. We hypothesize that the SiiE-MUC1 interaction positions the *Salmonella* T3SS needle close enough to the host membrane to inject its virulence factors and induce uptake.

<https://doi.org/10.1371/journal.ppat.1007566.g007>

(Fig 4) suggests that sialic acids on MUC1 are likely the primary target of SiiE. In colon, MUC1 is decorated with core 3 and core 4 glycostructures, with terminal fucoses or sialic acids [2,8] and this glycosylation pattern can be altered during *S. Typhimurium* infection [38]. In addition, MUC1 is upregulated under inflammatory conditions (Fig 3) [25,26] thereby increasing receptor availability. SiiE has been shown to contribute to *Salmonella* infections in mice. *S. Enteritidis* and *S. Typhimurium* strains lacking the SPI4 locus show a defect in intestinal colonization but are capable of establishing systemic infection [39].

A crucial aspect in the SiiE-MUC1 interaction is likely the structural architecture of both molecules. The SiiE protein is a giant adhesin (595 kDa) that contains an array of tandem repeats [37]. The extracellular domain of MUC1 also contains a (glycosylated) tandem repeat region. It can be imagined that the SiiE-MUC1 interaction involves sequential binding of the tandem repeats of both the adhesin and receptor. Such an interaction perfectly fits the need to breach the mucin barrier to correctly position the type III secretion system (T3SS) with its injectable virulence factors that are essential to initiate *Salmonella* invasion. It is important to consider that the MUC1 extracellular domain extends far from the plasma membrane and forms a barrier that is about 200–500 nm in size (6, 7). The T3SS injectosome, a needle-like machinery that is essential for successful invasion, is 80 nm in length [40]. Therefore, *Salmonella* needs additional virulence factors to breach the transmembrane mucin barrier and position the needle closer to the cell surface. SiiE has a rod-like structure and is 175 ± 5 nm in length [37]. Sequential interaction of the 53 highly conserved SiiE bacterial immunoglobulin (Blg) domains with the 42 highly glycosylated tandem repeats on MUC1 is likely a crucial first step to allow the T3SS system to initiate the invasion process. This scenario is supported by reports that increased deletion of the *Salmonella* SiiE Blg domains reduces bacterial invasion [41]. The mucus-binding protein MUB of *Lactobacillus reuteri* also contains multiple Blg-like repeats that bind intestinal mucus [42,43]. We hypothesize that SiiE interacts with MUC1 in a zipper-like manner (Fig 7B). Interaction of a single Blg domain with a single sialic acid is

probably of low affinity, but multivalency of the adhesin-sugar interactions will provide strong avidity. We observed that during *Salmonella* invasion, MUC1 is localized to cup-like structures that contain large clusters of *Salmonella*. It remains to be investigated if MUC1 plays an active or a passive role in cup formation and bacterial uptake. We hypothesize that the SiiE-MUC1 interaction positions the T3SS needle close enough to the cell surface to inject its virulence factors and induce ruffle formation and *Salmonella* uptake. It is tempting to speculate that a cycle of SiiE release and reattachment of a novel molecule would enable the bacteria to move closer to the epithelial cell surface. Our hypothesis extends the previously proposed model for the function of SiiE in *Salmonella* apical invasion by providing evidence that MUC1 serves as the receptor for the SiiE adhesin.

In conclusion, we demonstrate for the first time that the transmembrane mucin MUC1 facilitates *Salmonella* apical entry into intestinal epithelial cells and serves as a receptor for the *Salmonella* giant adhesin SiiE. The exploitation of MUC1 by *Salmonella* underlines the importance of transmembrane mucins as targets in bacterial pathogenesis.

Materials and methods

Bacterial strains and growth conditions

Salmonella enterica serovar Enteritidis (*S. Enteritidis*) (strain 90-13-706, CVI, Lelystad) was transformed with plasmid pTVmCherry carrying the *mCherry* gene of *Discosoma* sp. optimized for bacterial expression (generously provided by J.M. Wells, Wageningen University). *S. Enteritidis* strains CVI-1 and CVI-1 *invG* were described previously [44]. Both strains were transformed with the pJET-mCherry plasmid (a kind gift from Mark Wösten, Utrecht University). *Salmonella enterica* serovar Typhimurium (*S. Typhimurium*) SL1344 carrying plasmid pMW85 expressing GFP from a P_{pagC} promoter has been previously described [22,23]. *Salmonella* strains were routinely cultured at 37°C on LB agar plates containing kanamycin at 50 µg/ml or ampicillin at 100 µg/ml in 10 ml of LB broth while shaking (160 rpm). *Escherichia coli* DH5α used for cloning was grown on LB plates with the appropriate antibiotics.

Construction of the *Salmonella* Enteritidis *siiE* knockout strain

The *S. Enteritidis* *siiE* knockout strain was constructed by deletion of the *siiE* gene using the lambda red homologous recombination system [45] combined with flanking regions similar to a strategy that was previously published [19]. The two regions flanking the *SiiE* gene were amplified with primers (KS290 5'-GTAGCATGCCAAAGGTATAGAACTCAAAAAGG-GTATCTGGA-3' and KS291 5'-TACGGATCCACTCTCAAGGTGTATCTAATCGTTT AGT-3' and KS292 5'-GTAGGATC-CCTCACCTTTGGGTGAGGGGGTTTAC-3 and KS293 5'-TACGTC-GACCTTCTGAGATAAAAATATTCCTGTTCTTCT-GTCC-3') using the wild type *S. Enteritidis* genome DNA as a template and fused the respective sites of the spectinomycin adenyltransferase-encoding gene [46] using overlap extension PCR. The final product was ligated into the pKO3 vector carrying a chloramphenicol resistance gene and electroporated into *S. Enteritidis*. After recovery in SOC medium (1h, 30°C), the bacteria were plated on LB plates with chloramphenicol and incubated at 43°C. The next day, single colonies were suspended into 1 ml of LB broth, serially diluted, and immediately plated on 8% sucrose-spectinomycin plates and incubated at 30°C. Gene replacement was verified by PCR with primers KS295 5'-GTTTCATGGTCAGGGCGTTAT-3' and 452 5'-GGCTG-CTCAAACCTATAACCAC-3', 451 5'-AGGAGTATTAAAGCGAAGCAC-3' and KS296 5'-GGAAATACGGCCAGAGAC AAT-3' and KS295/KS296.

Mammalian cell lines and culture conditions

The human gastrointestinal epithelial cell lines HT29-MTX (a kind gift of Dr. Thécla Lesuffleur) [47], HT29-MTX- Δ MUC1 (derived from HT29-MTX wild type, this study), HT-29 (ATCC-HTB-38), Caco-2 (ATCC-HTB-37) and HRT-18 (ATCC-CCL-244) were routinely grown in 25 cm² flasks in Dulbecco's modified Eagle's medium (DMEM) containing 10% fetal calf serum (FCS) at 37°C in 5% CO₂. For *Salmonella* quantitative invasion assays, HT29-MTX wild type and Δ MUC1 cells were split into 12-well plates and grown for 5 days prior to addition of *Salmonella*. For microscopic cell imaging, cells were cultured on circular glass coverslips in 24-well plates.

Generation of the HT29-MTX Δ MUC1 cell line using CRISPR/Cas9

To generate a Δ MUC1 cell line, we used the pCRISPR-hCas9-2xgRNA-Puro plasmid [48] that encodes Cas9 with 2 guide RNAs to generate a 130 bp deletion in the 5' end of the MUC1 gene before the VNTR region. The pCRISPR plasmid was digested with *SapI* and simultaneously dephosphorylated with alkaline phosphatase (FastAP; ThermoFisher). Guide RNA primer sets A (KS36 5'-ACCGGGTCATGCAAGCTCTACCCC-3' and KS37 5'-AACGGGGTAGAGC TTGCATGACCC 3') and B (KS131 5'-CCGGACATCCTGTCCCTGAGTGGG-3' and KS132 5'-AAACCCACTCAGGGACAGGATGTC-3') were phosphorylated with T4 polynucleotide kinase (ThermoFisher) at 37°C for 30 min and annealed by cooling down from 85°C to 25°C at 0.1°C/sec. Annealed primer sets were ligated into the *SapI*-digested pCRISPR plasmid as confirmed by sequencing with primers KS46 5'-GTTACGCTAGTGCCAAGGTCCG-3' and KS47 5'-GAGTCAGTGAGCGAGGAAGC-3', resulting in plasmid pCR11. Two-day grown HT29-MTX cells were trypsinized from a 25 cm² flask and transfected in suspension with 2 μ g of pCR11, pCRISPR-empty or no plasmid using Fugene (Promega) according to the manufacturer's instructions. Cells were cultured in DMEM + 10% FCS for two days, after which 5 μ g/ml puromycin (Life Technologies) was added to the medium to select for positively transfected cells. Cells were maintained in medium with puromycin until all negative control cells had died. Single cell cloning was performed by serial dilution and single cell clones were tested for the MUC1 deletion by PCR with primers KS133 5'-CAGTCCTCCTGGTATTATTCTCTGGTG-3' and KS134 5'-CAGGTGGCAGCTGAACCTGAAG-3'. The absence of MUC1 protein in the HT29-MTX- Δ MUC1 cell line was confirmed by immunoblot with mouse monoclonal antibody 214D4 (a kind gift from Dr. John Hilken; CD227, Nordic MUBio) directed against the MUC1 tandem repeats.

Confocal microscopy

Cells were grown on cover slips (8 mm diameter #1.5) in 24-well plates and for bacterial invasion studies, *Salmonella* was grown as described below and added at a multiplicity of infection (MOI) of 60 for 1 h. Then cells were washed twice with Dulbecco's Phosphate Buffered Saline (DPBS, D8537, Sigma) and fixed with 4% cold paraformaldehyde in PBS (Affimetrix) for 30 min at room temperature. Cells were rinsed twice with DPBS before they were permeabilized in binding buffer (0.1% saponin, Sigma and 0.2% BSA, Sigma in DPBS) for 30 min. Next, coverslips were incubated with α -MUC1 antibody 214D4 at 1:150 dilution and/or α -SiiE rabbit polyclonal antiserum (1:200; a kind gift of Michael Hensel, University of Osnabrück) for 1h followed by 4 washing steps with binding buffer. The cover slips were incubated with Alexa Fluor-488/568-conjugated goat α -mouse IgG secondary antibodies (1:200; A11029, A11031; ThermoFisher), goat α -rabbit IgG secondary antibodies (1:200; A11034, A11036; ThermoFisher) and Alexa Fluor-647-conjugated donkey α -mouse IgG secondary antibody (1:200; 715-605-151; Jackson ImmunoResearch) and DAPI at 2 μ g/ml (D21490, Invitrogen) for 1h.

Coverslips were washed 3 times with DPBS, once with MilliQ, dried and embedded in Prolong diamond mounting solution (ThermoFisher) and allowed to harden. Images were collected on a Leica SPE-II confocal microscope using a 63x objective (NA 1.3, HCX PLANAPO oil) controlled by Leica LAS AF software with default settings to detect DAPI, Alexa488, Alexa568 and Alexa647. Axial series were collected with step sizes of 1 μm . Object centroid positions in Z were determined in IMARIS 8.2 (Bitplane, UK) on images that were deconvolved using the 3D automated deconvolution package in NIS elements (NIKON). *Salmonella* and SiiE segmented objects were created using the spot detection wizard and MUC1-labeled positions were isolated using the surface detection wizard in 5 image stacks. Centroid Z positions of the objects were extracted in the Vantage module and exported to Excel (Microsoft, Redmond USA) for plotting.

Quantitative invasion assay

Salmonella overnight cultures (16 h) were diluted 1:30 in LB broth and grown for 3.5 h at 37°C till late logarithmic phase. After adjustment of the OD₆₀₀ to 0.24, 1 ml of bacterial culture was centrifuged at 8000 rpm for 2 min. The bacterial pellet was resuspended in 1 ml DPBS, immediately 30 μl of bacterial suspension was added to cells in a 12-well plate in DMEM without FCS (MOI 15) and incubated for 1 h at 37°C. Cells were rinsed twice with DPBS, placed in DMEM without FCS containing 300 $\mu\text{g}/\text{mL}$ of gentamicin, and incubated for 1 h at 37°C to kill extracellular bacteria. Cells were then washed twice with DPBS and lysed with lysis buffer (0.1% Triton X-100 in DPBS) for 5 min at 37°C. Serial dilutions were made and plated on LB agar plates containing 50 $\mu\text{g}/\text{mL}$ kanamycin. The next day, colonies were counted.

Western blot

Protein samples were prepared from cells cultured in 6-wells plates. The cells were washed once with DPBS and 200 μl of lysis buffer was added to each well to detach the cells. Then 100 μl of 3x Laemmli sample buffer was added to the lysate followed by boiling for 5 min at 100°C. For immunoblotting of large mucin proteins, a Boric acid-Tris system was developed. A 5% mucin gel (12.5% 40% Acryl/Bis acryl, Biorad 161-0144; 26% 1.5 M Tris pH 8.8, Invitrogen; 10% SDS, Invitrogen; 10% ammonium persulfate, Invitrogen; 0.1% TEMED, ThermoFisher) was made in a Mini Protean II chamber (Bio-rad) using 1.5 mm spacer plates. Boiled protein lysates were loaded onto the gel, and run in Boric acid-Tris buffer (192 mM Boric acid, Merck; 1 mM EDTA, Merck; 0.1% SDS, to pH 7.6 with Tris) at 25 mA for 1.5 h. Protein was transferred onto a nitrocellulose membrane using a wet transfer system with transfer buffer (25 mM Tris; 192 mM glycine, Merck; 20% methanol, Merck) for 3 h at 90 V at 4°C. Subsequently, the membranes were blocked with 5% BSA in TSMT (20 mM Tris; 150 mM NaCl, Merck; 1 mM CaCl₂, Sigma; 2 mM MgCl₂, Merck; adjusted to pH 7 with HCl; 0.1% Tween 20, Sigma) overnight at 4°C. The next day, the membrane was incubated with 214D4 antibody at a dilution of 1:150 in TSMT containing 1% BSA for 1 h at RT, washed 2 times with TSMT, 2 times with DPBS and incubated with α -mouse IgG secondary antibody (A2304, Sigma) diluted 1:8000 in TSMT with 1% BSA for 1 h at RT. For detection of actin, cell lysates were loaded onto a 10% SDS-PAGE gel, transferred to PVDF membranes and incubated with α -Actin antibody (1:5,000; bs-0061R, Bioss) and α -rabbit IgG (1: 10,000; A4914, Sigma). Blots were developed with the Clarity Western ECL kit (Bio-Rad) and imaged in a Gel-Doc system (Bio-Rad).

Enzymatic removal of sialic acids

Desialylation of HT29-MTX and Δ MUC1 cells was achieved by incubating cells grown in a 24-well plate with 250 mU/mL neuraminidase (Sigma) in DPBS for 2 h at 37°C. Cells were then washed twice with DPBS and used in *Salmonella* invasion assays.

Supporting information

S1 Fig. (Accompanies Fig 1). (A) Single channel maximum projections with orthogonal view of the image depicted in Fig 1B and 1C. MUC1: green, *Salmonella*: red, nuclei: blue. (B) Montage of different Z planes of the image depicted in Fig 1B and 1C. MUC1: green, *Salmonella*: red, nuclei: blue. (C) Immunofluorescence confocal microscopy imaging of confluent HT29-MTX cells infected with *S. Enteritidis* CVI-1 wild type or *invG* knockout bacteria (mCherry, red) stained for MUC1 (214D4, green) and nuclei (DAPI, blue). White scale bars represent 20 μ m.

(TIF)

S2 Fig. (Accompanies Fig 6). Montage of different Z planes of the image depicted in Fig 6A. MUC1: white, SiiE: green, *Salmonella*: red, nuclei: blue.

(TIF)

S1 Movie. 3D projection and rotation of confocal microscopy image depicted in Fig 6A.

MUC1: white, SiiE: green, *Salmonella*: red, nuclei: blue.

(MOV)

Acknowledgments

We thank Rob Bleumink and Esther van 't Veld of the Center for Cell Imaging of the Utrecht Faculty of Veterinary Medicine for advice and assistance.

Author Contributions

Conceptualization: Karin Strijbis.

Investigation: Xinyue Li, Nancy M. C. Bleumink-Pluym, Yvette M. C. A. Luijkx, Richard W. Wubbolts.

Methodology: Xinyue Li, Richard W. Wubbolts, Karin Strijbis.

Software: Richard W. Wubbolts.

Supervision: Jos P. M. van Putten, Karin Strijbis.

Writing – original draft: Xinyue Li.

Writing – review & editing: Nancy M. C. Bleumink-Pluym, Yvette M. C. A. Luijkx, Jos P. M. van Putten, Karin Strijbis.

References

1. Johansson MEV, Sjövall H, Hansson GC. The gastrointestinal mucus system in health and disease. *Nat Rev Gastroenterol Hepatol*. Nature Publishing Group; 2013; 10: 352–361. <https://doi.org/10.1038/nrgastro.2013.35> PMID: 23478383
2. Tailford LE, Crost EH, Kavanaugh D, Juge N. Mucin glycan foraging in the human gut microbiome. *Front Genet*. 2015; 6: 1–18.

3. Van Putten JPM, Strijbis K. Transmembrane Mucins: Signaling Receptors at the Intersection of Inflammation and Cancer. *J Innate Immun.* 2017; 9: 281–299. <https://doi.org/10.1159/000453594> PMID: 28052300
4. Ogata S, Uehara H, Chen A, Itzkowitz SH. Mucin gene expression in colonic tissues and cell lines. *Cancer Res.* 1992; 52: 5971–5978. Available: <http://www.ncbi.nlm.nih.gov/pubmed/1394223> PMID: 1394223
5. Ho SB, Niehans GA, Lyftogt C, Yan PS, Cherwitz DL, Gum ET, et al. Heterogeneity of mucin gene expression in normal and neoplastic tissues. *Cancer Res.* 1993; 53: 641–651. PMID: 7678777
6. Jentoft N. Why are proteins O-mannosylated? *Trends Biochem Sci.* 1990; 15: 291–294.
7. Hilkens J, Ligtenberg MJL, Vos HL, Litvinov S V. Cell membrane-associated mucins and their adhesion-modulating property. *Trends Biochem Sci.* 1992; 17: 359–363. [https://doi.org/10.1016/0968-0004\(92\)90315-Z](https://doi.org/10.1016/0968-0004(92)90315-Z) PMID: 1412714
8. Brockhausen I, Schachter H, Stanley P. O-GalNAc Glycans. *Essentials of Glycobiology* 2nd edition Chapter 9. Cold Spring Harbor Laboratory Press; 2009.
9. Spicer AP, Parry G, Patton S, Gendler SJ. Molecular cloning and analysis of the mouse homologue of the tumor-associated mucin, MUC1, reveals conservation of potential O-glycosylation sites, transmembrane, and cytoplasmic domains and a loss of minisatellite-like polymorphism. *J Biol Chem.* 1991; 266: 15099–15109. Available: <http://www.ncbi.nlm.nih.gov/pubmed/1714452> PMID: 1714452
10. Lindén SK, Sheng YH, Every AL, Miles KM, Skoog EC, Florin THJ, et al. MUC1 limits *Helicobacter pylori* infection both by steric hindrance and by acting as a releasable decoy. *PLoS Pathog.* 2009; 5: e1000617. <https://doi.org/10.1371/journal.ppat.1000617> PMID: 19816567
11. McAuley JL, Linden SK, Chin WP, King RM, Pennington HL, Gendler SJ, et al. MUC1 cell surface mucin is a critical element of the mucosal barrier to infection. *J Clin Invest.* 2007; 117: 2313–2324. <https://doi.org/10.1172/JCI26705> PMID: 17641781
12. McGuckin MA, Every AL, Skene CD, Linden SK, Chionh YT, Swierczak A, et al. Muc1 mucin limits both *Helicobacter pylori* colonization of the murine gastric mucosa and associated gastritis. *Gastroenterology.* 2007; 133: 1210–1218. <https://doi.org/10.1053/j.gastro.2007.07.003> PMID: 17919495
13. Walters RW, Pilewski JM, Chiorini JA, Zabner J. Secreted and transmembrane mucins inhibit gene transfer with AAV4 more efficiently than AAV5. *J Biol Chem.* 2002; 277: 23709–23713. <https://doi.org/10.1074/jbc.M200292200> PMID: 11925433
14. Arcasoy SM, Latoche J, Gondor M, Watkins SC, Henderson RA, Hughey R, et al. MUC1 and other sialoglycoconjugates inhibit adenovirus-mediated gene transfer to epithelial cells. *Am J Respir Cell Mol Biol.* 1997; 17: 422–435. <https://doi.org/10.1165/ajrcmb.17.4.2714> PMID: 9376117
15. McAuley JL, Corcilus L, Tan HX, Payne RJ, McGuckin MA, Brown LE. The cell surface mucin MUC1 limits the severity of influenza A virus infection. *Mucosal Immunol.* Nature Publishing Group; 2017; 10: 1581–1593. <https://doi.org/10.1038/mi.2017.16> PMID: 28327617
16. Larock DL, Chaudhary A, Miller SI. Salmonellae interactions with host processes. *Nat Rev Microbiol.* Nature Publishing Group; 2015; 13: 191–205. <https://doi.org/10.1038/nrmicro3420> PMID: 25749450
17. Sansonetti PJ. War and peace at mucosal surfaces. *Nat Rev Immunol.* 2004; 4: 953–964. <https://doi.org/10.1038/nri1499> PMID: 15573130
18. Pinaud L, Sansonetti PJ, Phalipon A. Host Cell Targeting by Enteropathogenic Bacteria T3SS Effectors. *Trends Microbiol.* 2018; 26: 266–283. <https://doi.org/10.1016/j.tim.2018.01.010> PMID: 29477730
19. Gerlach RG, Jäckel D, Stecher B, Wagner C, Lupas A, Hardt WD, et al. *Salmonella* Pathogenicity Island 4 encodes a giant non-fimbrial adhesin and the cognate type 1 secretion system. *Cell Microbiol.* 2007; 9: 1834–1850. <https://doi.org/10.1111/j.1462-5822.2007.00919.x> PMID: 17388786
20. Wagner C, Barlag B, Gerlach RG, Deiwick J, Hensel M. The *Salmonella enterica* giant adhesin SiiE binds to polarized epithelial cells in a lectin-like manner. *Cell Microbiol.* 2014; 16: 962–975. <https://doi.org/10.1111/cmi.12253> PMID: 24345213
21. Gagnon M, Zihler Berner A, Chervet N, Chassard C, Lacroix C. Comparison of the Caco-2, HT-29 and the mucus-secreting HT29-MTX intestinal cell models to investigate *Salmonella* adhesion and invasion. *J Microbiol Methods.* Elsevier B.V.; 2013; 94: 274–279. <https://doi.org/10.1016/j.mimet.2013.06.027> PMID: 23835135
22. Bouwman LI, de Zoete MR, Bleumink-Pluym NMC, Flavell RA, van Putten JPM. Inflammasome Activation by *Campylobacter jejuni*. *J Immunol.* 2014; 193: 4548–4557. <https://doi.org/10.4049/jimmunol.1400648> PMID: 25267974
23. Bumann D. Regulated antigen expression in live recombinant *Salmonella enterica* serovar Typhimurium strongly affects colonization capabilities and specific CD4(+)-T-cell responses. *Infect Immun.* American Society for Microbiology (ASM); 2001; 69: 7493–7500. <https://doi.org/10.1128/IAI.69.12.7493-7500.2001>

24. Lorkowski M, Felipe-López A, Danzer CA, Hansmeier N, Hensel M. *Salmonella enterica* invasion of polarized epithelial cells is a highly cooperative effort. *Infect Immun*. 2014; 82: 2657–2667. <https://doi.org/10.1128/IAI.00023-14> PMID: 24711567
25. Linden SK, Sutton P, Karlsson NG, Korolik V, McGuckin MA. Mucins in the mucosal barrier to infection. *Mucosal Immunol*. 2008; 1: 183–197. <https://doi.org/10.1038/mi.2008.5> PMID: 19079178
26. Li Y-Y, Hsieh L-L, Tang R-P, Liao S-K, Yeh K-Y. Macrophage-derived interleukin-6 up-regulates MUC1, but down-regulates MUC2 expression in the human colon cancer HT-29 cell line. *Cell Immunol*. 2009; 256: 19–26. <https://doi.org/10.1016/j.cellimm.2009.01.001> PMID: 19201396
27. Wagner C, Barlag B, Gerlach RG, Deiwick J, Hensel M. The *Salmonella enterica* giant adhesin SiiE binds to polarized epithelial cells in a lectin-like manner. *Cell Microbiol*. 2014; 16: 962–975. <https://doi.org/10.1111/cmi.12253> PMID: 24345213
28. Gipson IK, Spurr-Michaud S, Tisdale A, Menon BB. Comparison of the transmembrane mucins MUC1 and MUC16 in epithelial barrier function. *Batra SK, editor. PLoS One*. 2014; 9: e100393. <https://doi.org/10.1371/journal.pone.0100393> PMID: 24968021
29. Jones BD, Ghori N, Falkow S. *Salmonella typhimurium* initiates murine infection by penetrating and destroying the specialized epithelial M cells of the Peyer's patches. *J Exp Med*. 1994; 180: 15–23. <https://doi.org/10.1084/jem.180.1.15> PMID: 8006579
30. Marchetti M, Sirard JC, Sansonetti P, Pringault E, Kernéis S. Interaction of pathogenic bacteria with rabbit appendix M cells: bacterial motility is a key feature in vivo. *Microbes Infect*. 2004; 6: 521–528. <https://doi.org/10.1016/j.micinf.2004.02.009> PMID: 15158184
31. Watson PR, Paulin SM, Bland AP, Jones PW, Wallis TS. Characterization of intestinal invasion by *Salmonella typhimurium* and *Salmonella dublin* and effect of a mutation in the invH gene. *Infect Immun*. 1995; 63: 2743–2754. Available: <http://www.ncbi.nlm.nih.gov/pubmed/7790093> PMID: 7790093
32. Bolton AJ, Wallis TS, Osborne MP, Stephen J. Interaction of *Salmonella choleraesuis*, *Salmonella dublin* and *Salmonella typhimurium* with porcine and bovine terminal ileum in vivo. *Microbiology*. *Microbiology Society*; 1999; 145: 2431–2441. <https://doi.org/10.1099/00221287-145-9-2431> PMID: 10517596
33. Bolton AJ, Martin GD, Osborne MP, Wallis TS, Stephen J. Invasiveness of *Salmonella* serotypes Typhimurium, Choleraesuis and Dublin for rabbit terminal ileum in vitro. *J Med Microbiol*. 1999; 48: 801–810. <https://doi.org/10.1099/00222615-48-9-801> PMID: 10482290
34. Robbe C, Capon C, Coddeville B, Michalski J-C. Structural diversity and specific distribution of O-glycans in normal human mucins along the intestinal tract. *Biochem J*. 2004; 384: 307–316. <https://doi.org/10.1042/BJ20040605> PMID: 15361072
35. Holmen Larsson JM, Thomsson KA, Rodriguez-Pineiro AM, Karlsson H, Hansson GC. Studies of mucus in mouse stomach, small intestine, and colon. III. Gastrointestinal Muc5ac and Muc2 mucin O-glycan patterns reveal a regiospecific distribution. *AJP Gastrointest Liver Physiol*. 2013; 305: G357–G363. <https://doi.org/10.1152/ajpgi.00048.2013> PMID: 23832516
36. Barlag B, Hensel M. The giant adhesin SiiE of *Salmonella enterica*. *Molecules*. 2015; 20: 1134–1150. <https://doi.org/10.3390/molecules20011134> PMID: 25587788
37. Wagner C, Polke M, Gerlach RG, Linke D, Stierhof Y-D, Schwarz H, et al. Functional dissection of SiiE, a giant non-fimbrial adhesin of *Salmonella enterica*. *Cell Microbiol*. 2011; 13: 1286–1301. <https://doi.org/10.1111/j.1462-5822.2011.01621.x> PMID: 21729227
38. Arabyan N, Park D, Foutouhi S, Weis AM, Huang BC, Williams CC, et al. *Salmonella* Degrades the Host Glycocalyx Leading to Altered Infection and Glycan Remodeling. *Sci Rep*. 2016; 6: 29525. <https://doi.org/10.1038/srep29525> PMID: 27389966
39. Kiss T, Morgan E, Nagy G. Contribution of SPI-4 genes to the virulence of *Salmonella enterica*. *FEMS Microbiol Lett*. 2007; 275: 153–159. <https://doi.org/10.1111/j.1574-6968.2007.00871.x> PMID: 17711458
40. Kubori T, Matsushima Y, Nakamura D, Uralil J, Lara-Tejero M, Sukhan A, et al. Supramolecular Structure of the *Salmonella typhimurium* Type III Protein Secretion System. *Science (80-)*. 1998; 280: 602–605. <https://doi.org/10.1126/science.280.5363.602>
41. Gerlach RG, Cláudio N, Rohde M, Jäckel D, Wagner C, Hensel M. Cooperation of *Salmonella* pathogenicity islands 1 and 4 is required to breach epithelial barriers. *Cell Microbiol*. 2008; 10: 2364–2376. <https://doi.org/10.1111/j.1462-5822.2008.01218.x> PMID: 18671822
42. MacKenzie DA, Tailford LE, Hemmings AM, Juge N. Crystal structure of a mucus-binding protein repeat reveals an unexpected functional immunoglobulin binding activity. *J Biol Chem*. 2009; 284: 32444–32453. <https://doi.org/10.1074/jbc.M109.040907> PMID: 19758995
43. Etzold S, Kober OI, Mackenzie DA, Tailford LE, Gunning AP, Walshaw J, et al. Structural basis for adaptation of lactobacilli to gastrointestinal mucus. *Environ Microbiol*. 2014; 16: 888–903. <https://doi.org/10.1111/1462-2920.12377> PMID: 24373178

44. Zhao Y, Jansen R, Gaastra W, Arkesteijn G, van der Zeijst BAM, van Putten JPM. Identification of genes affecting *Salmonella enterica* serovar enteritidis infection of chicken macrophages. *Infect Immun*. 2002; 70: 5319–21. Available: <http://www.ncbi.nlm.nih.gov/pubmed/12183592> <https://doi.org/10.1128/IAI.70.9.5319-5321.2002> PMID: 12183592
45. Link AJ, Phillips D, Church GM. Methods for generating precise deletions and insertions in the genome of wild-type *Escherichia coli*: application to open reading frame characterization. *J Bacteriol*. 1997; 179: 6228–6237. Available: <http://www.ncbi.nlm.nih.gov/pubmed/9335267> PMID: 9335267
46. Zhou W, Wang Y, Lin J. Functional Cloning and Characterization of Antibiotic Resistance Genes from the Chicken Gut Microbiome. *Appl Environ Microbiol*. 2012; 78: 3028–3032. <https://doi.org/10.1128/AEM.06920-11> PMID: 22286984
47. Lesuffleur T, Porchet N, Aubert JP, Swallow D, Gum JR, Kim YS, et al. Differential expression of the human mucin genes MUC1 to MUC5 in relation to growth and differentiation of different mucus-secreting HT-29 cell subpopulations. *J Cell Sci*. 1993; 106: 771–783. Available: <http://www.ncbi.nlm.nih.gov/pubmed/8308060> PMID: 8308060
48. Langereis MA, Rabouw HH, Holwerda M, Visser LJ, van Kuppeveld FJM. Knockout of cGAS and STING Rescues Virus Infection of Plasmid DNA-Transfected Cells. Perlman S, editor. *J Virol*. 2015; 89: 11169–11173. <https://doi.org/10.1128/JVI.01781-15> PMID: 26311870